Supplemental Material for "Laterally resolved small-angle scattering intensity from lipid bilayer simulations: an exact and a limited-range treatment"

Mitchell W. Dorrell,[†,‡] Frederick A. Heberle,[¶] John Katsaras,[§,‖] Lutz Maibaum,[⊥] Edward Lyman,[‡,#] and Alexander J. Sodt[*,†]

†*Eunice Kennedy Shriver National Institute of Child Health and Human Development, Bethesda, MD, USA.*

‡*Department of Physics and Astronomy, University of Delaware, Newark, DE, USA.*

¶*Department of Chemistry, University of Tennessee, Knoxville, TN, USA.*

§*Biology and Soft Matter Division, Oak Ridge National Laboratory, Oak Ridge, TN, USA.*

‖*Department of Physics and Astronomy, University of Tennessee, Knoxville, TN, USA.*

⊥*Department of Chemistry, University of Washington, Seattle, Wa, USA.*

#*Department of Chemistry and Biochemistry, University of Delaware, Newark, DE, USA.*

E-mail: alexander.sodt@nih.gov

Contents

S1 Scattering

The scattering problem is typically posed by applying a perturbation $V(\boldsymbol{r})$ to the free particle Hamiltonian $\frac{p^2}{2m}$ as:

$$H = \frac{p^2}{2m} + \lambda V(\boldsymbol{r}), \tag{S1}$$

where λ is the coupling parameter for the subsequent perturbation theory. The un-normalized solution to $\hat{H}_0\psi_0(\boldsymbol{r}) = E_0\psi_0(\boldsymbol{r})$ is

$$\psi_0(\boldsymbol{r}) = e^{\imath \boldsymbol{k}\cdot\boldsymbol{r}}. \tag{S2}$$

Perturbation theory is then applied through first order in λ to yield:

$$\psi(\boldsymbol{r}) = \psi_0(\boldsymbol{r}) + \frac{-2m}{4\pi\hbar^2}\int \mathrm{d}^3\boldsymbol{r}' V(\boldsymbol{r}')\psi_0(\boldsymbol{r}')\frac{e^{\imath k|\boldsymbol{r}-\boldsymbol{r}'|}}{|\boldsymbol{r}-\boldsymbol{r}'|} + \mathcal{O}[\lambda^2]. \tag{S3}$$

See, for example Eq. 7.1.9 of Ref.[1]

S1.1 Neutron scattering

Consider the atomic nucleus as a point scatterer as its dimensions are much smaller than the neutron wavelength (Å scale). Mathematically for nucleus a the potential is approximated as a Dirac delta function (δ) with magnitude v_a,

$$V_a(\boldsymbol{r}') = v_a\delta(\boldsymbol{r}' - \boldsymbol{r}_a). \tag{S4}$$

In analogy with classical scatterers, v_a can be rewritten as

$$v_a = b_a\frac{4\pi\hbar^2}{2m}, \tag{S5}$$

where b_a functions as the classical scattering length.

Evaluating Eq. S3 for $\psi(\boldsymbol{r})$ at the detector position $\boldsymbol{r}_{\mathrm{D}}$ a distance r_{D} away, yields:

$$\psi(\boldsymbol{r}) \approx e^{\imath \boldsymbol{k}\cdot\boldsymbol{r}_{\mathrm{D}}} - b_a \frac{e^{\imath k|\boldsymbol{r}_{\mathrm{D}}-\boldsymbol{r}_a|}}{|\boldsymbol{r}_{\mathrm{D}}-\boldsymbol{r}_a|} e^{\imath \boldsymbol{k}\cdot\boldsymbol{r}_a}. \tag{S6}$$

Breaking down $\psi(\boldsymbol{r}_{\mathrm{D}})$ in Eq. S6 yields a factor of $e^{\imath \boldsymbol{k}\cdot\boldsymbol{r}_a}$ due to the phase accumulated by the incoming neutron beam (this depends on the beam orientation $\boldsymbol{k}$ and the position of the nucleus $\boldsymbol{r}_a$) and a factor due to the spherically scattered neutron $e^{\imath k|\boldsymbol{r}_{\mathrm{D}}-\boldsymbol{r}_a|}$. The sign of the phase of the scattered neutron may flip depending if the nuclear potential (v_a) is net repulsive or attractive. Finally, the wavefunction of the scattered piece attenuates with the distance from the nucleus to the detector. The $e^{\imath \boldsymbol{k}\cdot\boldsymbol{r}_{\mathrm{D}}}$ term represents the signal of the unscattered neutron beam and dwarfs the scattered signal. The source neutron beam is limited so that only scattered neutrons reach the detectors.

The point approximation of the potential of a single nucleus yields a spherically symmetric scatterer; the amplitude is the same in all directions. The unit vector to a point on the detector is $\hat{\boldsymbol{r}}_{\mathrm{D}}$. Later, this will also be described as the scattering direction, which for elastic scattering, is

$$\boldsymbol{k}' = |\boldsymbol{k}|\hat{\boldsymbol{r}}_{\mathrm{D}} = k\hat{\boldsymbol{r}}_{\mathrm{D}}. \tag{S7}$$

Summing the scattering from multiple nuclei interfering at the detector reflects the internal geometry of the collection of nuclei in the sample. The sum is facilitated by approximating the distance to the detector by:

$$|\boldsymbol{r}_{\mathrm{D}} - \boldsymbol{r}_a| \approx r_{\mathrm{D}} - \hat{\boldsymbol{r}}_{\mathrm{D}} \cdot \boldsymbol{r}_a, \tag{S8}$$

valid for $r_{\mathrm{D}} \gg r_a$. Accounting for a collection of nuclei $\{\boldsymbol{r}_a\}$, and to first order in r_{D}^{-1},

$$\begin{aligned}\psi(\boldsymbol{r}_{\mathrm{D}}) &= -\frac{1}{r_{\mathrm{D}}} e^{\imath k r_{\mathrm{D}}} \sum_a b_a e^{-\imath k \hat{\boldsymbol{r}}_{\mathrm{D}} \cdot \boldsymbol{r}_a} e^{\imath \boldsymbol{k} \cdot \boldsymbol{r}_a} \\ &= -\frac{1}{r_{\mathrm{D}}} e^{\imath k r_{\mathrm{D}}} \sum_a b_a e^{\imath (\boldsymbol{k} - \boldsymbol{k}') \cdot \boldsymbol{r}_a}, \end{aligned} \tag{S9}$$

where the second line follows from Eq. S7.

From Eq. S9, the interference between neutrons scattered from different sites a and b depends on the difference $(\boldsymbol{k} - \boldsymbol{k}') \cdot (\boldsymbol{r}_b - \boldsymbol{r}_a)$, not on the absolute value of k. For convenience the vector $\boldsymbol{q} = \boldsymbol{k} - \boldsymbol{k}'$ is defined to quantify this vector. The signal at the detector now only depends on the nuclei of the sample, $\{\boldsymbol{r}_a\}$ through $\boldsymbol{q}$:

$$\psi(\boldsymbol{r}_{\mathrm{D}}) = -\frac{1}{r_{\mathrm{D}}} e^{\imath k r_{\mathrm{D}}} \sum_a b_a e^{\imath \boldsymbol{q} \cdot \boldsymbol{r}_a}, \tag{S10}$$

$$|\psi(\boldsymbol{r}_{\mathrm{D}})|^2 = (\frac{1}{r_{\mathrm{D}}})^2 \sum_{a,b} b_a b_b e^{\imath \boldsymbol{q} \cdot (\boldsymbol{r}_a - \boldsymbol{r}_b)}. \tag{S11}$$

Only the magnitude, and not the interference pattern itself, depends on r_{D}.

Given that scattering from the nucleus is equally likely in every direction it is worth considering why the signal typically appears strongest along the beam path. In this case the scattered wavevector $\boldsymbol{k}'$ differs only slightly from $\boldsymbol{k}$. Particles will interfere constructively at the detector when

$$e^{\imath (\boldsymbol{k} - \boldsymbol{k}') \cdot \boldsymbol{r}_a} \approx 1, \tag{S12}$$

for the particles in the sample. This will be true, in general, for $\boldsymbol{k} - \boldsymbol{k}'$ much less than the sample dimension. For sufficiently small $\boldsymbol{k} - \boldsymbol{k}'$, the finite spread of $\boldsymbol{r}_a$ will only sample the central maximum of $e^{\imath (\boldsymbol{k} - \boldsymbol{k}') \cdot \boldsymbol{r}_a}$, leading to purely constructive interference. For larger $\boldsymbol{k} - \boldsymbol{k}'$, the exponential will oscillate fast enough that the spread in $\boldsymbol{r}_a$ can now sample minima as well as maxima, leading to destructive interference and significantly less signal. Thus the enhanced scattering at small angles reflects the lengthscale of the sample, and not an

inherent likelihood of small momentum transfer.

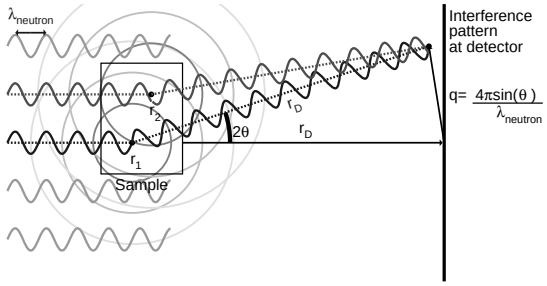

Figure S1: An idealized schematic of the SANS experiment. Not shown is the possibility of the sign of the scattered wave reversing due to scattering (e.g., for hydrogen).

Shown in Fig. S1 is an idealization of the SANS experiment. The phase relevant to interference at the detector can be computed from two paths. First, from the neutron source to particle $\boldsymbol{r}_1$ the neutron accumulates phase $e^{\imath \boldsymbol{k}\cdot\boldsymbol{r}_1}$ before it scatters (relative to a particle at the origin). It then undergoes elastic scattering such that $|\boldsymbol{k}'| = |\boldsymbol{k}|$. The scattered neutron travels to the detector, accumulating phase factor $e^{-\imath \boldsymbol{k}'\cdot\boldsymbol{r}_1}$ (also relative to a particle scattering from the origin).

Whether the wavefunction at the detector is proportional to $e^{\imath \boldsymbol{q}\cdot\boldsymbol{r}}$ or $e^{-\imath \boldsymbol{q}\cdot\boldsymbol{r}}$ is irrelevant. This paper applies the convention $e^{-\imath \boldsymbol{q}}$.

S2 Solvent Subtraction

First let us consider a system of finite size in all dimensions and small enough to fit within a single simulation box, such as a protein or micelle. For this system, the x-, y-, and z-axes are interchangeable. Furthermore, all six sides of the simulation box (the periodic boundaries) are located entirely in bulk solvent, which means the discontinuity in the neutron scattering length density at the edge of the system is the same at every periodic boundary. The symmetry allows the discontinuity to be removed using an analytical correction to the scattering intensity expression. An arbitrary value can be subtracted from the neutron scattering length density for all space without affecting the scattering intensity:

$$I(\boldsymbol{q}) = \lim_{L\to\infty} \underbrace{\int \mathrm{d}^3\boldsymbol{r}_1 \int \mathrm{d}^3\boldsymbol{r}_2}_{\substack{\text{from } -L \text{ to } L \\ \text{in all dimensions}}} (\beta(\boldsymbol{r}_1)+\beta_\mathrm{w})(\beta(\boldsymbol{r}_2)+\beta_\mathrm{w}) e^{-\imath\boldsymbol{q}\cdot(\boldsymbol{r}_2-\boldsymbol{r}_1)} \tag{S13}$$

$$= \lim_{L\to\infty} \frac{1}{(8L^3)^2} \left(\int \mathrm{d}^3\boldsymbol{r}_1 \int \mathrm{d}^3\boldsymbol{r}_2 \beta(\boldsymbol{r}_1)\beta(\boldsymbol{r}_2) e^{-\imath\boldsymbol{q}\cdot(\boldsymbol{r}_2-\boldsymbol{r}_1)} + {\beta_\mathrm{w}}^2 \int \mathrm{d}^3\boldsymbol{r}_1 \int \mathrm{d}^3\boldsymbol{r}_2 e^{-\imath\boldsymbol{q}\cdot(\boldsymbol{r}_2-\boldsymbol{r}_1)} \right.$$
$$\left. + 2\left\{ \beta_\mathrm{w} \int \mathrm{d}^3\boldsymbol{r}_1 \int \mathrm{d}^3\boldsymbol{r}_2 \beta(\boldsymbol{r}_2) e^{-\imath\boldsymbol{q}\cdot(\boldsymbol{r}_2-\boldsymbol{r}_1)} \right\} \right) \tag{S14}$$

Terms with a factor equivalent to $\int_{-L}^{L} e^{-\imath\boldsymbol{q}\cdot\boldsymbol{r}}$, for example,

$$\beta_\mathrm{w} \int \mathrm{d}^3\boldsymbol{r}_1 e^{-\imath\boldsymbol{q}\cdot\boldsymbol{r}_1} \, \mathrm{d}^3\boldsymbol{r}_2 e^{-\imath\boldsymbol{q}\cdot\boldsymbol{r}_2} \beta(\boldsymbol{r}_2) \tag{S15}$$

evaluate to be proportional to $2q^{-1}\sin(Lq)$. That is, these terms oscillate with increasing frequency around a zero mean as L grows large. This, naturally, is simply the scattering from a very large shape whose size L, is reflected by the feature $\Delta q = \frac{1}{L}$. For very large samples, this is too small to be resolved and reduces to the average value, zero.

The case of a bilayer, simulated with periodic boundary conditions in z, makes it desirable to not include the z periodic images, as they would spuriously contribute a feature from the

perfect lamellar spacing. This results in a solvent discontinuity at the boundary. Since the problematic discontinuity is caused by the non-physical neutron scattering length density of "vacuum" outside of the simulation box, it makes sense to change the density in this region (all space except for the interior of the simulation box) to the density of the bulk solvent. If we then subtract the density of the bulk solvent (a constant) from all space, we only affect the scattering intensity at $I(0)$. This is mathematically equivalent to subtracting the neutron scattering length density of the bulk solvent from just the interior of the simulation box, while leaving the space outside of the simulation box untouched as vacuum. This subtraction neatly brings the neutron scattering length density at the faces of the simulation box to zero, creating a smooth transition from simulated system to vacuum. The subtraction of this term can be resolved as separate integrals which are evaluated analytically.

$$I(\boldsymbol{q}) = \left| \int \mathrm{d}^3\boldsymbol{r} (\beta(\boldsymbol{r}) - \beta_\mathrm{w}) e^{-\imath \boldsymbol{q}\cdot\boldsymbol{r}} \right|^2 = \left| \int \mathrm{d}^3\boldsymbol{r} \beta(\boldsymbol{r}) e^{-\imath \boldsymbol{q}\cdot\boldsymbol{r}} - \beta_\mathrm{w} \int \mathrm{d}^3\boldsymbol{r} e^{-\imath \boldsymbol{q}\cdot\boldsymbol{r}} \right|^2, \tag{S16}$$

$$I(\boldsymbol{q}) = \left| \sum_i b_i e^{-\imath \boldsymbol{q}\cdot\boldsymbol{r}_i} - \beta_\mathrm{w} V \operatorname{sinc}\left(\frac{L_x q_x}{2}\right) \operatorname{sinc}\left(\frac{L_y q_y}{2}\right) \operatorname{sinc}\left(\frac{L_z q_z}{2}\right) \right|^2, \tag{S17}$$

where L_x, L_y, and L_z are the x-, y-, and z-dimensions of the simulation box, and $V = L_x L_y L_z$ is the volume of the simulation box.

S3 Mathematical supplement and justifications

S3.1 Auto-correlation function

The expression

$$\int_{-\infty}^{\infty} dz \beta(z) \beta(z + \Delta z) \tag{S18}$$

is equivalent to an auto-correlation function in space. Writing $\beta(z)$ in terms of its Fourier transform with the split $(2\pi)^{-1}$ convention:

$$\beta(z) = (2\pi)^{-\frac{1}{2}} \int_{-\infty}^{\infty} dq \tilde{\beta}(q) e^{\imath q z} \tag{S19}$$

yields

$$\begin{aligned}
\int_{-\infty}^{\infty} dz \beta(z)\beta(z+\Delta z) &= (2\pi)^{-1} \int_{-\infty}^{\infty} dz \int_{-\infty}^{\infty} dq' \int_{-\infty}^{\infty} dq'' \tilde{\beta}(q')\tilde{\beta}(q'') e^{\imath q' z} e^{\imath q'' z} e^{\imath q'' \Delta z}, \\
&= (2\pi)^{-1} \int_{-\infty}^{\infty} dq' \int_{-\infty}^{\infty} dq'' \tilde{\beta}(q'')\tilde{\beta}(q') e^{\imath q'' \Delta z} \int_{-\infty}^{\infty} dz e^{\imath q' z} e^{\imath q'' z}, \\
&= \int_{-\infty}^{\infty} dq' \int_{-\infty}^{\infty} dq'' \tilde{\beta}(q'')\tilde{\beta}(q') e^{\imath q'' \Delta z} \delta(q' + q''), \\
&= \int_{-\infty}^{\infty} dq' |\tilde{\beta}(q')|^2 e^{-\imath q' \Delta z}.
\end{aligned} \tag{S20}$$

where

$$\int_{-\infty}^{\infty} dz e^{\imath q' z} e^{\imath q'' z} = 2\pi \delta(q' + q''), \tag{S21}$$

and, since $\tilde{\beta}$ is a Fourier transform of a real function,

$$\tilde{\beta}(-q') = \tilde{\beta}^*(q'). \tag{S22}$$

S3.2 Derivation of orientational averaging of Dirac brush

The orientational average of the periodically replicated simulation cell is computed as:

$$\begin{aligned}
\frac{1}{4\pi q^2} \int_{-q}^{q} \mathrm{d}q'_x \int_{-\sqrt{q^2 - {q'_x}^2}}^{\sqrt{q^2 - {q'_x}^2}} \mathrm{d}q'_y \int_{-\sqrt{q^2 - {q'_x}^2 - {q'_y}^2}}^{\sqrt{q^2 - {q'_x}^2 - {q'_y}^2}} \mathrm{d}q'_z \delta(q - \sqrt{{q'_x}^2 + {q'_y}^2 + {q'_z}^2}) \times \\
\frac{2\pi}{L_x} \mathrm{III}_{\frac{2\pi}{L_x}}(q'_x) \frac{2\pi}{L_y} \mathrm{III}_{\frac{2\pi}{L_y}}(q'_y) |I_0(q'_x, q'_y, q'_z)|^2,
\end{aligned} \tag{S23}$$

where $|I_0(q'_x, q'_y, q'_z)|^2$ is the single unit cell amplitude squared. The leading normalization $\frac{1}{4\pi q^2}$ accounts for the q-dependence of transforming from an integral over angles to q vectors.

The initial integral over q_z is performed by using:

$$\delta(g(q'_z)) = \sum_{q'_{z,0}|g(q'_{z,0})=0} \frac{\delta(q'_z - q'_{z,0})}{|g'(q'_{z,0})|}, \tag{S24}$$

where g' is the derivative of g and $q_{z,0}$ is a root of $g(q_z)$. In this case $g(q'_z) = q - \sqrt{{q'_x}^2 + {q'_y}^2 + {q'_z}^2}$ and $g'(q'_z) = -\frac{q'_z}{\sqrt{{q'_x}^2+{q'_y}^2+{q'_z}^2}}$. The Dirac delta function becomes

$$\delta\big(q - \sqrt{{q'_x}^2 + {q'_y}^2 + {q'_z}^2}\big) = q\frac{\delta(q'_z - \sqrt{q^2 - {q'_x}^2 - {q'_y}^2}) + \delta(q'_z + \sqrt{q^2 - {q'_x}^2 - {q'_y}^2})}{\sqrt{q^2 - {q'_x}^2 - {q'_y}^2}}. \tag{S25}$$

For brevity, we rewrite this in terms of just the positive root, and label that root using the unprimed $q_z = \sqrt{q^2 - {q'_x}^2 - {q'_y}^2}$:

$$\delta\big(q - \sqrt{{q'_x}^2 + {q'_y}^2 + {q'_z}^2}\big) = q\frac{\delta(q'_z - q_z) + \delta(q'_z + q_z)}{q_z}. \tag{S26}$$

The integral becomes:

$$\frac{\pi}{L_x L_y}\int_{-q}^{q} \mathrm{d}q'_x \int_{-\sqrt{q^2-{q'_x}^2}}^{\sqrt{q^2-{q'_x}^2}} \mathrm{d}q'_y \, \mathrm{III}_{\frac{2\pi}{L_x}}(q'_x)\, \mathrm{III}_{\frac{2\pi}{L_y}}(q'_y) \frac{|I_0(q'_x, q'_y, q_z)|^2 + |I_0(q'_x, q'_y, -q_z)|^2}{q q_z}, \tag{S27}$$

where q_z retains its implicit dependence on q'_x and q'_y. The remaining comb functions now select q'_x and q'_y such that they fall on a $\frac{2\pi}{L_x}$-by-$\frac{2\pi}{L_y}$-spaced grid, while the bounds of integration constrain $\sqrt{{q'_x}^2 + {q'_y}^2 + q_z^2} \leq q$:

$$I_\Omega(q) = \frac{\pi}{L_x L_y} \sum_{m=\lceil -qL_x/2\pi \rceil}^{\lfloor qL_x/2\pi \rfloor} \sum_{n=\left\lceil -\sqrt{(L_y q/2\pi)^2 - (\frac{L_y}{L_x}m)^2} \right\rceil}^{\left\lfloor \sqrt{(L_y q/2\pi)^2 - (\frac{L_y}{L_x}m)^2} \right\rfloor} \frac{I_1(q_x, q_y, q_z) + I_1(q_x, q_y, -q_z)}{q\, q_z}, \tag{S28}$$

with unprimed $q_x = \frac{2\pi m}{L_x}$ and $q_y = \frac{2\pi n}{L_y}$. Figure S2 illustrates the particular values of the vector $\boldsymbol{q} = \{q_x, q_y, q_z\}$ satisfying the constraints of the comb. In the limit $q \to 0$, q_z is equal

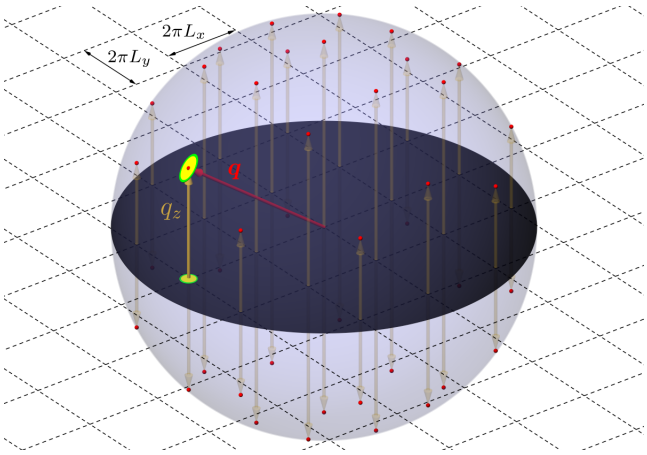

Figure S2: An illustration of the $\{q_x, q_y, q_z\}$ vectors, with magnitude $|\boldsymbol{q}|$, that satisfy the constraints of the q_x and q_y comb functions. The grid lines cutting through the middle of the sphere at $q_z = 0$ show the values of q_x and q_y for which the comb is equivalent to the Dirac delta function. The intersection of q_x and q_y grid lines are the points for which both comb functions are valid. Tracking up or down in q_z to the sphere of radius q provides the value of q_z.

to q, and $\frac{2\pi I_1(0)}{L_x L_y}$ reduces to $2\pi \frac{A}{(2+1)N(2+1)M}\bar{b}^2$. Removing the "per-unit-cell" normalization by multiplying by $(2+1)N(2+1)M$ yields the asymptotic expression, $2\pi A q^{-2}\bar{b}^2$, consistent with lateral averaging.

S4 Explicit calculation of PFFT terms

The asymmetry in the integration domains imparts a conceptual asymmetry to the product of binomials in the integrand. By expanding the product, we can consider each term separately.

$$I_\Omega(q) = \int_{\text{cell}} \mathrm{d}^3\boldsymbol{r}_1 \int_{z_2\in\text{cell}} \mathrm{d}^3\boldsymbol{r}_2 \Big(\underbrace{\beta_{\text{sys}}(\boldsymbol{r}_1)\beta_{\text{sys}}(\boldsymbol{r}_2)}_{\textbf{I}} - \underbrace{\beta_{\text{w}}\beta_{\text{sys}}(\boldsymbol{r}_1)}_{\textbf{II}} - \underbrace{\beta_{\text{w}}\beta_{\text{sys}}(\boldsymbol{r}_2)}_{\textbf{III}} + \underbrace{{\beta_{\text{w}}}^2}_{\textbf{IV}} \Big) \operatorname{sinc}(q|\boldsymbol{r}_1 - \boldsymbol{r}_2|). \tag{S29}$$

Each term corresponds to a specific correlation between two regions.

- **I** Correlations between a single cell of the simulation and the infinite bilayer model (both particulate and continuum models contribute to this term).

- **II** Correlations between a single cell of the simulation and the infinite solvent background.

- **III** Correlations between a single cell of solvent background and the infinite bilayer model.

- **IV** Correlations between a single cell of solvent background and the infinite solvent background.

The first step in evaluating any of the terms is to define $\boldsymbol{r}_\Delta = \boldsymbol{r}_2 - \boldsymbol{r}_1$ and use this to rewrite the $\boldsymbol{r}_2$ integration in terms of $\boldsymbol{r}_\Delta$.

$$I_\Omega(q) = \int_{\text{cell}} \mathrm{d}^3\boldsymbol{r}_1 \int_{z_\Delta + z_1 \in \text{cell}} \mathrm{d}^3\boldsymbol{r}_\Delta \Big(\underbrace{\beta_{\text{sys}}(\boldsymbol{r}_1)\beta_{\text{sys}}(\boldsymbol{r}_\Delta + \boldsymbol{r}_1)}_{\mathbf{I}} - \underbrace{\beta_{\text{w}}\beta_{\text{sys}}(\boldsymbol{r}_1)}_{\mathbf{II}} - \underbrace{\beta_{\text{w}}\beta_{\text{sys}}(\boldsymbol{r}_\Delta + \boldsymbol{r}_1)}_{\mathbf{III}} + \underbrace{{\beta_{\text{w}}}^2}_{\mathbf{IV}} \Big) \operatorname{sinc}(qr_\Delta). \tag{S30}$$

In term **I**, the system will be decomposed into the near-field and far-field models to exclude unphysical long-range correlations. The PFFT cutoff defines a cylindrical region around each scattering element. This region needs to be recentered on each scatterer exactly once, so $\beta_{\text{sys}}(\boldsymbol{r}_1)$ is used for the reference elements to limit that integration domain to one instance of the simulation cell. Since the reference element is trivially always within the PFFT cutoff, the particulate form is substituted.

$$I_{\mathbf{I}}(q) = \int_{\text{cell}} \mathrm{d}^3\boldsymbol{r}_1 \int_{z_\Delta + z_1 \in \text{cell}} \mathrm{d}^3\boldsymbol{r}_\Delta \beta_{\text{part}}(\boldsymbol{r}_1)\beta_{\text{sys}}(\boldsymbol{r}_\Delta + \boldsymbol{r}_1) \operatorname{sinc}(qr_\Delta). \tag{S31}$$

The domain of the $\boldsymbol{r}_\Delta$ integral can be divided into two regions by the PFFT cylinder around $\boldsymbol{r}_1$. The cylinder has radius r_c and extends from the lower boundary of the simulation cell to the upper boundary. When integrating over these two regions separately, the term integrating inside the cylinder will be labeled **Ia**, and the term integrating outside the cylinder will be labeled **Ib**. In the interior region, $\beta_{\text{sys}}(\boldsymbol{r}_\Delta + \boldsymbol{r}_1)$ will take the particulate form, and in the

exterior region it will take the continuum (LA) form.

$$I_{\mathbf{I}}(q) = \int_{\text{cell}} \mathrm{d}^3\boldsymbol{r}_1 \beta_{\text{part}}(\boldsymbol{r}_1) \Bigg(\underbrace{\int_{\boldsymbol{r}_\Delta \in \text{cyl}} \mathrm{d}^3\boldsymbol{r}_\Delta \beta_{\text{part}}(\boldsymbol{r}_\Delta + \boldsymbol{r}_1) \operatorname{sinc}(q r_\Delta)}_{\mathbf{Ia}} + \underbrace{\int_{\substack{\boldsymbol{r}_\Delta \notin \text{cyl} \\ z_\Delta + z_1 \in \text{cell}}} \mathrm{d}^3\boldsymbol{r}_\Delta \beta_{\text{LA}}(z_\Delta + z_1) \operatorname{sinc}(q r_\Delta)}_{\mathbf{Ib}} \Bigg). \tag{S32}$$

For term **Ia**, the explicit form for β_{part} from is used to evaluate the integral.

$$I_{\mathbf{Ia}}(q) = \int_{\text{cell}} \mathrm{d}^3\boldsymbol{r}_1 \left(\sum_i b_i \delta(\boldsymbol{r}_1 - \boldsymbol{r}_i) \right) \int_{\boldsymbol{r}_\Delta \in \text{cyl}} \mathrm{d}^3\boldsymbol{r}_\Delta \left(\sum_j b_j \delta(\boldsymbol{r}_\Delta + \boldsymbol{r}_1 - \boldsymbol{r}_j) \right) \operatorname{sinc}(q r_\Delta), \tag{S33}$$

$$I_{\mathbf{Ia}}(q) = \sum_{\substack{i \in \text{cell} \\ j \in \text{cyl}}} b_i b_j \operatorname{sinc}(q|\boldsymbol{r}_j - \boldsymbol{r}_i|). \tag{S34}$$

Alternatively, the $\boldsymbol{r}_\Delta$ integration may be delayed and reduced to a one-dimensional integral (the motivation will become clear after the other terms are discussed):

$$I_{\mathbf{Ia}}(q) = \sum_{\substack{i \in \text{cell} \\ j \in \text{cyl}}} b_i b_j \int_0^\infty \mathrm{d}r_\Delta \delta(r_\Delta - |\boldsymbol{r}_j - \boldsymbol{r}_i|) \operatorname{sinc}(q r_\Delta). \tag{S35}$$

For term **Ib**, the explicit form for $\beta_{\text{part}}(\boldsymbol{r}_1)$ will again be substituted into the expression

$$I_{\mathbf{Ib}}(q) = \sum_{i \in \text{cell}} b_i \int_{\substack{\boldsymbol{r}_\Delta \notin \text{cyl} \\ z_\Delta + z_i \in \text{cell}}} \mathrm{d}^3\boldsymbol{r}_\Delta \beta_{\text{LA}}(z_\Delta + z_i) \operatorname{sinc}(q r_\Delta). \tag{S36}$$

The integrand can be partially evaluated by expressing $\boldsymbol{r}_\Delta$ in spherical polar coordinates, such that $z_\Delta = r_\Delta \cos(\phi)$. The integration over the azimuth angle trivially yields a factor of 2π.

$$I_{\mathbf{Ib}}(q) = 2\pi \sum_{i \in \text{cell}} b_i \int_{r_c}^\infty \mathrm{d}r_\Delta \int_{\max[\phi_-, \phi_c]}^{\min[\phi_+, \pi - \phi_c]} \mathrm{d}\phi \beta_{\text{LA}}(r_\Delta \cos(\phi) + z_i) {r_\Delta}^2 \sin(\phi) \operatorname{sinc}(q r_\Delta), \tag{S37}$$

where the ϕ integration bounds have been chosen to observe both constraints on the integration domain, all points outside the r_c cylindrical cutoff ($r_\Delta \sin(\phi) > r_c$, which implies $\phi_c < \phi < \pi - \phi_c$) but still inside the upper and lower boundaries of the simulation cell ($\phi_- < \phi < \phi_+$), where ϕ_c corresponds to the minimum angle to exceed the r_c cutoff and ϕ_- and ϕ_+ correspond to the the upper and lower boundaries of the simulation cell, z_+ and z_-:

$$\phi_c = \arcsin(r_c/r_\Delta), \tag{S38}$$

$$\phi_\mp = \arccos((z_\pm - z_i)/r_\Delta). \tag{S39}$$

Optionally, another change-of-variables may make this expression more intuitive. With $z_2 = r_\Delta \cos(\phi) + z_i$, we can change the ϕ integral back into a z integral:

$$I_{\mathbf{Ib}}(q) = 2\pi \sum_{i \in \text{cell}} b_i \int_{r_c}^{\infty} \mathrm{d}r_\Delta \int_{\max[z_-, z_i - \sqrt{{r_\Delta}^2 - {r_c}^2}]}^{\min[z_+, z_i + \sqrt{{r_\Delta}^2 - {r_c}^2}]} \mathrm{d}z_2 \beta_{\mathrm{LA}}(z_2) r_\Delta \operatorname{sinc}(q r_\Delta). \tag{S40}$$

With term **II**, the particulate form will no longer be used. In isolation, the term is expressed:

$$I_{\mathbf{II}}(q) = -\beta_{\mathrm{w}} \int_{\text{cell}} \mathrm{d}^3\boldsymbol{r}_1 \int_{z_\Delta + z_1 \in \text{cell}} \mathrm{d}^3\boldsymbol{r}_\Delta \beta_{\mathrm{sys}}(\boldsymbol{r}_1) \operatorname{sinc}(q r_\Delta). \tag{S41}$$

The $\boldsymbol{r}_\Delta$ integration is performed in spherical polar coordinates with the same definitions used above in term **Ib**:

$$I_{\mathbf{II}}(q) = -2\pi\beta_{\mathrm{w}} \int_{\text{cell}} \mathrm{d}^3\boldsymbol{r}_1 \int_0^{\infty} \mathrm{d}r_\Delta \int_{\phi_-}^{\phi_+} \mathrm{d}\phi {r_\Delta}^2 \sin(\phi) \beta_{\mathrm{sys}}(\boldsymbol{r}_1) \operatorname{sinc}(q r_\Delta). \tag{S42}$$

The integrand has no dependence on x_1 and y_1 outside of $\beta_{\mathrm{sys}}(\boldsymbol{r}_1)$, which allows us to use the definition of $\beta_{\mathrm{LA}}(z)$ from to resolve the integration over those variables.

$$I_{\mathbf{II}}(q) = -2\pi L_x L_y \beta_{\mathrm{w}} \int_{z_-}^{z_+} \mathrm{d}z_1 \int_0^{\infty} \mathrm{d}r_\Delta \int_{\phi_-}^{\phi_+} \mathrm{d}\phi {r_\Delta}^2 \sin(\phi) \beta_{\mathrm{LA}}(z_1) \operatorname{sinc}(q r_\Delta). \tag{S43}$$

The ϕ integration is straightforward, yielding a factor of $z_+ - z_- = L_z$.

$$I_{\mathbf{II}}(q) = -2\pi L_x L_y L_z \beta_{\mathrm{w}} \int_{z_-}^{z_+} \mathrm{d}z_1 \int_0^{\infty} \mathrm{d}r_\Delta r_\Delta \beta_{\mathrm{LA}}(z_1)\,\mathrm{sinc}(q r_\Delta). \tag{S44}$$

Term **III** is conceptually different from term **II** because term **II** represented finite system and infinite solvent while term **III** represents finite solvent and infinite system. However, recall that the scattering intensity per simulation cell was derived from the total scattering by limiting one of the integration domains to a single simulation cell. For a finite number of cells (N), consider the relation

$$\begin{aligned} I_\Omega(q) &= \int_{1\mathrm{cell}} \mathrm{d}^3\boldsymbol{r}_1 \int_{N\mathrm{cells}} \mathrm{d}^3\boldsymbol{r}_2 f(\boldsymbol{r}_1, \boldsymbol{r}_2) = \frac{1}{N} \int_{N\mathrm{cells}} \mathrm{d}^3\boldsymbol{r}_1 \int_{N\mathrm{cells}} \mathrm{d}^3\boldsymbol{r}_2 f(\boldsymbol{r}_1, \boldsymbol{r}_2) \\ &= \int_{N\mathrm{cells}} \mathrm{d}^3\boldsymbol{r}_1 \int_{1\mathrm{cell}} \mathrm{d}^3\boldsymbol{r}_2 f(\boldsymbol{r}_1, \boldsymbol{r}_2) = \int_{N\mathrm{cells}} \mathrm{d}^3\boldsymbol{r}_2 \int_{1\mathrm{cell}} \mathrm{d}^3\boldsymbol{r}_1 f(\boldsymbol{r}_2, \boldsymbol{r}_1), \end{aligned}$$

where the $1/N$ division is applied to the $\boldsymbol{r}_2$ integration instead of $\boldsymbol{r}_1$, and the labels are swapped at the end. Since terms **II** and **III** differ only in having swapped variables in the integrand, the above relation shows that they are equivalent:

$$I_{\mathbf{III}}(q) = I_{\mathbf{II}}(q). \tag{S45}$$

Term **IV** has the simplest evaluation, since both density factors are constant.

$$I_{\mathbf{IV}}(q) = {\beta_{\mathrm{w}}}^2 \int_{\mathrm{cell}} \mathrm{d}^3\boldsymbol{r}_1 \int_{z_\Delta + z_1 \in \mathrm{cell}} \mathrm{d}^3\boldsymbol{r}_\Delta\,\mathrm{sinc}(q r_\Delta). \tag{S46}$$

The $\boldsymbol{r}_\Delta$ integration is again expressed in spherical polar coordinates, and the ϕ integral is

again resolved to a factor of L_z.

$$I_{\mathbf{IV}}(q) = 2\pi {\beta_{\mathrm{w}}}^2 \int_{\mathrm{cell}} \mathrm{d}^3\boldsymbol{r}_1 \int_{\phi_-}^{\phi_+} \mathrm{d}\phi \int_0^\infty \mathrm{d}r_\Delta {r_\Delta}^2 \sin(\phi)\,\mathrm{sinc}(qr_\Delta) \tag{S47}$$

$$= 2\pi L_z {\beta_{\mathrm{w}}}^2 \int_{\mathrm{cell}} \mathrm{d}^3\boldsymbol{r}_1 \int_0^\infty \mathrm{d}r_\Delta r_\Delta\,\mathrm{sinc}(qr_\Delta). \tag{S48}$$

The integrand has no dependence on $\boldsymbol{r}_1$, so that integral contributes a factor of $L_x L_y L_z$:

$$I_{\mathbf{IV}}(q) = 2\pi L_x L_y {L_z}^2 {\beta_{\mathrm{w}}}^2 \int_0^\infty \mathrm{d}r_\Delta r_\Delta\,\mathrm{sinc}(qr_\Delta). \tag{S49}$$

To summarize, the full set of terms is expressed below.

$$I_{\mathbf{Ia}}(q) = \sum_{\substack{i\in\mathrm{cell}\\ j\in\mathrm{cyl}}} b_i b_j\,\mathrm{sinc}(qr_\Delta) = \sum_{\substack{i\in\mathrm{cell}\\ j\in\mathrm{cyl}}} b_i b_j \int_0^\infty \mathrm{d}r_\Delta \delta(r_\Delta - |\boldsymbol{r}_j - \boldsymbol{r}_i|)\,\mathrm{sinc}(qr_\Delta), \tag{S50}$$

$$I_{\mathbf{Ib}}(q) = 2\pi \sum_{i\in\mathrm{cell}} b_i \int_{r_c}^\infty \mathrm{d}r_\Delta \int_{\max[\phi_-,\phi_c]}^{\min[\phi_+,\pi-\phi_c]} \mathrm{d}\phi \beta_{\mathrm{LA}}(r_\Delta\cos(\phi) + z_i){r_\Delta}^2 \sin(\phi)\,\mathrm{sinc}(qr_\Delta), \tag{S51}$$

$$I_{\mathbf{II}}(q) = I_{\mathbf{III}}(q) = -2\pi L_x L_y L_z \beta_{\mathrm{w}} \int_{z_-}^{z_+} \mathrm{d}z_1 \int_0^\infty \mathrm{d}r_\Delta r_\Delta \beta_{\mathrm{LA}}(z_1)\,\mathrm{sinc}(qr_\Delta), \tag{S52}$$

$$I_{\mathbf{IV}}(q) = 2\pi L_x L_y {L_z}^2 {\beta_{\mathrm{w}}}^2 \int_0^\infty \mathrm{d}r_\Delta r_\Delta\,\mathrm{sinc}(qr_\Delta). \tag{S53}$$

All of these terms involve an integration over r_Δ (using the alternative form of term **Ia**).

S5 Scattering lengths used for Martini beads

References

(1) Sakurai, J. J. *Modern Quantum Mechanics*; Addison-Wesley, 1994.

Table S1: Scattering lengths used to model Martini lipids. For the matrix lipids, the middle two acyl beads (e.g., C2, D3) use the scattering of 'D' beads, regardless of identity.

Martini atom	Scattering length ($10^{-12}cm$)
NC3	-0.5158
PO4	2.672
GL	1.88805
C	-0.3332
D	0.4152
W	-0.672